

Interfacial conduction in ionically conducting two-phase materials: Calculations using the grain consolidation model

Bo Nettelblad, Bin Zhu, and Bengt-Erik Mellander

Department of Physics, Chalmers University of Technology, S-412 96 Gothenburg, Sweden

(Received 17 May 1996)

We have used the grain consolidation model to study the ionic conductivity in different two-phase composite systems where interfacial conductivity is assumed to be causing a conductivity enhancement. The model predicts results that are qualitatively similar to experimental data, displaying sharp “knees” in the composition dependence. We have modeled materials consisting of grains in a host background where the grain size is either constant or varying with concentration. The model can explain even unusual behavior such as the existence of both a maximum and a minimum in conductivity at intermediate compositions. To achieve this we had to assume that the grains become smaller as their volume fraction increases. [S0163-1829(97)00209-9]

I. INTRODUCTION

Composite ionic conductors have been widely studied since the discovery that adding an alumina phase to a moderately conducting material may cause a considerable enhancement of the conductivity.¹⁻¹² A plot of the ionic conductivity versus alumina content shows a peak at intermediate alumina concentrations; for LiI-Al₂O₃ the peak occurs at about 30–40 vol % Al₂O₃.¹ This enhancement is often explained as an interface effect where the ionic conductivity is larger at the solid-solid interfaces than in the bulk of either material and it has been shown that the conductivity increases with decreasing size of the alumina grains—a good example is given by Kumar and Shahi.¹² A similar conductivity enhancement has also been observed for two-phase systems consisting of two moderately conducting phases.⁷ For binary systems with a eutectic point the grain size in the two-phase region is strongly dependent on the composition if the samples have been prepared from the melt. A conductivity enhancement has been observed also in such systems; the maximum conductivity is in this case obtained at the fine-grained eutectic composition.¹³ However, it has also been shown that if a material with very high ionic conductivity is mixed with alumina the conductivity decreases with increasing amount of alumina over the entire composition range.⁹

Another type of inhomogeneous system that has been thoroughly investigated is solid porous materials impregnated with a liquid.¹⁴⁻²¹ Examples of such materials are high-voltage electrical insulators and porous sandstone impregnated with salty water. Also for these composites, interface effects at the solid-liquid interface are important for the electrical properties. Simulations of the electrical properties of packs of nonoverlapping hard spheres, covered by an interfacial layer, were made by Schwartz, Carboczi, and Bentz²¹ as a way of modeling the electrical properties of cement mortar. Another model, which permits overlapping, or truncated spheres, forming a continuous phase, is the so-called grain consolidation model (GCM). This model has been successfully used for estimations of the electrical properties of solid-liquid composites.²²⁻²⁶ Originally, this model

was proposed for two-phase systems,²²⁻²³ but it has been extended to systems with special interface properties.²⁴⁻²⁶

In this paper, the grain consolidation model is used to simulate the ionic conduction in ionic conducting composite materials with enhanced interface conductivity. We compare the effects of using different assumptions on grain growth; we also discuss the differences that occur when one of the components is an insulator versus the case when both components are conducting. We compare the simulated results with experimental data reported in the literature and with measured values for the KNO₃-Al₂O₃ and RbNO₃-Al₂O₃ systems. These materials have high ionic and protonic conductivities, 10⁻² to 1 S/cm at intermediate temperatures (400–600 °C) and have been used as electrolytes in intermediate temperature fuel cells.^{27,28}

II. EXPERIMENTAL

The nitrate salt-alumina composites are two-phase materials that are somewhat similar in structure to the composite insulating systems described above. At high temperature the nitrate salts are molten, thus these materials may be described as a solid ceramic matrix containing a molten phase.

RbNO₃ and KNO₃ (p.a., Merck, Germany) and alumina (Merck, Germany) were mixed in various molar ratios and ground thoroughly. The ground mixtures were sintered at 450 °C for more than 12 h. The sintered products were ground, pressed as a tablet, and heated again in the same way as the first time. The sintering and grinding caused a rearrangement of the particle size in the sample and in the final samples the grain size actually decreased with increasing amount of alumina.

The ionic conductivities of the samples were determined using complex impedance spectra measured by a computerized LCR meter (Hewlett-Packard HP 4274 A). The bulk conductivity was determined from the intersection of the high-frequency semicircle and the real axis in the complex impedance plot. Platinum paste (Leitplatin 308A, Hanau, Germany) applied to the flat surfaces of the cylindrical samples were used as electrodes.

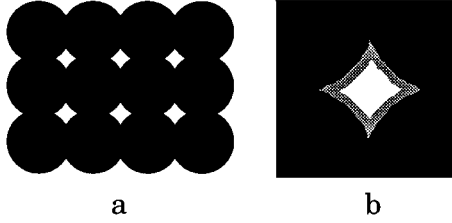


FIG. 1. (a) Cross section of one layer in the sc lattice for the grain consolidation model. (b) The model of the interface including an interface layer (not necessarily drawn to scale).

III. THEORETICAL BACKGROUND

We assume that the maximum often found in plots of conductivity vs composition is due to interface conduction. We regard the composite as solid particles with a conducting shell immersed in a continuous conducting host material. If the particles are insulating, the conduction is hindered when the amount of insulating material is increased, but the total interface area also increases. If the interface conductivity is high this might actually lead to an increase in the effective conductivity of the inhomogeneous material. However, as the volume fraction of the solid is increased further, the solid particles begin to agglomerate, and the interface area is decreased.

The grain consolidation model was proposed by Roberts and Schwartz.²² In this simple structural model, one of the phases is initially considered to consist of spherical grains. For the simplest case, it is assumed that the grains are equal in size and placed on a regular lattice, but the model has been extended to the more general case of a given initial grain size distribution as well as a random configuration.^{22,23} The grains are then allowed to grow equally in all directions (except where they touch each other if the grains are considered to be noninterpenetrable) until the desired value of the pore volume fraction is attained [see Fig. 1(a)]. This treatment actually bears some resemblance to the cementation process in natural sedimentary rock.²² It should be pointed out that it is also possible to let the spheres grow inhomogeneously in different directions.²³

This model has several attractive features. In real porous materials it is often found that the pore space remains interconnected down to very low values of porosity (pore volume fraction), and that is the case also for this model. If one starts with equal-sized grains on a body-centered-cubic lattice, the pores are interconnected down to the porosity 0.0055. Another advantage with the GCM model is that it is relatively simple to perform calculations of the properties of this “composite” when spheres of equal size placed on a regular lattice are used. It can be noted that this model has also been used for predictions of fluid permeability.²⁹

Shen *et al.*³⁰ developed a useful method for the Fourier space calculation of the conductivity of a composite consisting of equal spheres placed on a regular lattice. To achieve faster convergence, they separated the electric field, \mathbf{E} into two terms:

$$\mathbf{E} = \mathbf{E}_1(\mathbf{r})\theta_1(\mathbf{r}) + \mathbf{E}_2(\mathbf{r})\theta_2(\mathbf{r}), \quad (1)$$

where $\theta_1(\mathbf{r})$ equals one in material 1 and zero in material 2 [and the reverse for $\theta_2(\mathbf{r})$]. Accordingly, the values of $\mathbf{E}_1(\mathbf{r})$

in material 2 and of $\mathbf{E}_2(\mathbf{r})$ in material 1 are of no interest, and these functions can be smooth. Thus, fewer Fourier terms are needed to get a good approximation. As is shown in Refs. 30 and 31, second- or even first-order approximation gives good results.

The \mathbf{E} and θ functions can be expressed in Fourier series:

$$\mathbf{E}_1(\mathbf{r}) = \sum_{\mathbf{m}} C_{1\mathbf{m}} e^{j\mathbf{b}_{\mathbf{m}} \cdot \mathbf{r}}, \quad \theta_1(\mathbf{r}) = \sum_{\mathbf{m}} T_{1\mathbf{m}} e^{j\mathbf{b}_{\mathbf{m}} \cdot \mathbf{r}}, \quad (2)$$

where $\mathbf{b}_{\mathbf{m}}$ is $2\pi/a$ times the vector $[m_1, m_2, m_3]$, (m_1, m_2 and m_3 are the coordinates in reciprocal space) and a is the distance between the centers of neighboring grains.

Maxwell’s equations can then be written as

$$\mathbf{b}_{\mathbf{n}} \times \sum_{\alpha} \sum_{\mathbf{m}} T_{\alpha\mathbf{n}-\mathbf{m}} \mathbf{C}_{\alpha\mathbf{m}} = 0, \quad (3a)$$

$$\mathbf{b}_{\mathbf{n}} \sum_{\alpha} \sum_{\mathbf{m}} \sigma_{\alpha} T_{\alpha\mathbf{n}-\mathbf{m}} \mathbf{C}_{\alpha\mathbf{m}} = 0, \quad (3b)$$

where α denotes summation over the two phases. From these equations, and the condition that the spatial average of the electric field is equal to the applied field, the unknown \mathbf{C} components can be calculated. The equations can only be solved for a finite number of equations and unknowns; the maximum value of the components of \mathbf{m} defines the number of unknowns and the maximum value of the components of \mathbf{n} defines the number of equations. Shen *et al.*³⁰ recommend that the order of \mathbf{n} should exceed the order of the calculated Fourier components of the field, \mathbf{m} , by at least 2. This gives more equations than unknowns, and the whole system of equations is solved by a least-squares approximation. The \mathbf{C} components then give the effective conductivity (the effective dielectric constant can be calculated analogously):

$$\sigma_{\text{eff},j} = \frac{1}{\mathbf{E}_{0j}} \sum_{\alpha} \sum_{\mathbf{m}} \sigma_{\alpha} T_{\alpha 0-\mathbf{m}} (\mathbf{C}_{\alpha\mathbf{m}} \cdot \mathbf{e}_j). \quad (4)$$

The T components are determined by the geometry; for non-touching spheres, an analytical determination is possible,³⁰ while numerical integration is needed for touching spheres.

We have previously^{25,26} extended this model to calculations of the frequency-dependent complex dielectric constant of a two-phase medium. In the present study as well as in some earlier articles we considered the interface layer to be a third phase, that could have different electrical properties than either the solid or the bulk liquid, to account for interface conduction or diffusion effects. The third phase was treated in the same way as the other two phases in all calculations. (In a previous paper on sedimentary rock Tyc *et al.*²⁴ added a third layer to account for clay particles at the interface.) We also used this method to calculate the distribution of the electric field between the phases.³² (A different calculation method for periodic structures was used by Sareni *et al.*³³)

The factor σ makes Eq. (3b) differently weighted in the least-squares calculations than Eq. (3a). We solved this problem²⁶ by dividing Eq. (3b) with $|\sigma_1 - \sigma_2|$. We have also found that errors could be obtained in the estimated field within the lower-conductivity phase if the conductivities of the two phases differ much.³² Even if each phase is homo-

geneous and isotropic, we may obtain sources in the electric field within the low-conductivity phase. Since we are only calculating a finite number of Fourier terms, and using more equations than unknowns, the errors in the estimated field can become large even if the errors in the product $\sigma \cdot \mathbf{E}$ are small. This problem was solved by adding the equations:

$$\theta_1(\mathbf{r})[\nabla \cdot \mathbf{E}_1(\mathbf{r})] = 0, \quad (5)$$

which take into account the fact that the field \mathbf{E}_1 is not necessarily source-free outside material 1. (It was here assumed that material 1 has the lower conductivity.) We extended this method to a situation including an interface layer, as is shown in Fig. 1(b).^{25,26}

IV. CALCULATION CONDITIONS

We assumed that one of the phases form equal particles that are placed on a lattice. For low relative volume fractions of this phase, the particles are spherical and suspended in the host phase, but for higher volume fractions, the particles form a continuous phase of truncated spheres. In general, we assumed that the particles are nonconducting, but we also included a calculation where the conductivity of the particles is equal to that of the host phase.

In most cases the particles were placed on a body-centered-cubic (bcc) lattice. For touching spheres in an bcc lattice, the volume fraction of spheres is 0.68, whereas the corresponding values for the simple cubic (sc) and the face-centered-cubic (fcc) lattices are 0.52 and 0.74. Batchelor and O'Brien³⁴ reported values for random sphere packings of 0.60 to 0.64, i.e., close to the value for the bcc lattice; Scott and Kilgour³⁵ measured on 80 000 steel balls in a container that had been subjected to mechanical vibrations and arrived at the result 0.6366. Of the cubic lattices, the bcc lattice thus appears to be closest to random packings, but we performed the calculations also for the sc and fcc lattices for comparison.

We also included an interface layer, and we assumed that the properties of this layer were independent of the relative volume fractions of the constituent phases. We accordingly assumed an interface layer of finite, constant thickness, and constant conductivity. It is then clear that an increase in relative volume fractions of the particle-forming phase can proceed in at least two different ways: Either, the number of particles is constant and their size increases, or the size of the particles is constant and their number increases. Normalizing all lengths to the size of the unit cell (Wigner-Seitz cell) surrounding each particle, we see that in the first case, the thickness of the interface layer (relative to the unit-cell size) is constant, while the thickness in the second case is proportional to the radius of the particles.

Both these models for increase in particle volume fractions have some questionable implications. Assuming a constant number of particles would at very low volume fraction of particles yield a finite volume of interface layer. This volume would not tend to zero as the volume of particles tends to zero. Furthermore, if we assume that the radius of the spheres is kept constant, we note that the volume of each particle is constant as long as the particles do not touch. For touching particles, the volume is lower than for untouching particles.

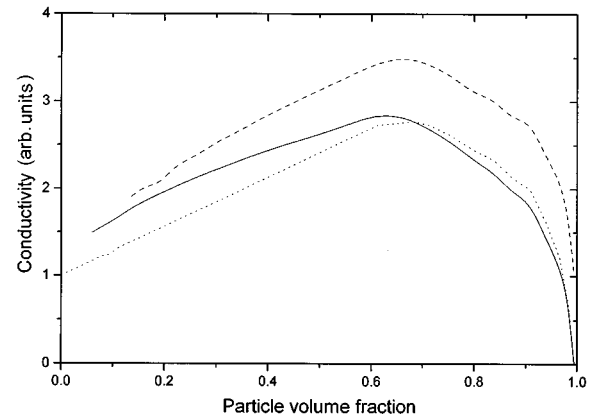


FIG. 2. Results from GCM calculations assuming constant number of conducting particles (dashed line), constant number of nonconducting particles (solid line), and nonconducting particles of constant radius (dotted line).

A further complication is that in real samples the grain size is strongly affected by the sample preparation method; if the samples are prepared from the melt a very fine-grained material can be obtained if the composition is close to a eutectic composition, grain growth may occur at elevated temperatures, etc. Thus the grain size may be dependent on composition and may, e.g., decrease with increasing particle volume fraction.

In this paper, we performed calculations, both assuming a constant number of particles, as well as a constant particle radius. We also performed calculations assuming that the radius of the particles decreases as their volume fraction increases; those calculations are discussed more below.

In our initial calculations we used a model where the conductivity of the interface layer was 55 times higher than in the host phase but this figure was decreased to 15 for the case when the particle radius decreases with increasing particle volume fraction. The thickness of the interface layer was 0.01 times the size of the unit cell of the bcc lattice at the point where the spheres touch each other (the thickness of the layer was either constant, or proportional to the particle radius, but we deliberately let these two cases yield the same result at the point where the spheres exactly touch). We either let the particles be insulating, or have the same conductivity as the host phase.

V. RESULTS AND DISCUSSION

In Fig. 2, we show the conductivity of the model composite material as a function of the volume fraction of particles. Results are shown for three different systems: assuming conducting particles growing in such a way that the number of particles is kept constant, assuming nonconducting particles growing similarly, and assuming nonconducting particles, with constant radius, but increasing their number as their volume fraction is increased. All these simulations were made using identical particles placed on a bcc lattice.

A striking characteristic of these curves is that they consist of almost linear parts, joined at sharp “knees.” Similar “knees” are, in fact, often found in experimental data, for example for LiI-Al₂O₃ (Ref. 1) and RbCl-Al₂O₃.¹² In the model the knees occur when the spheres start to intersect.

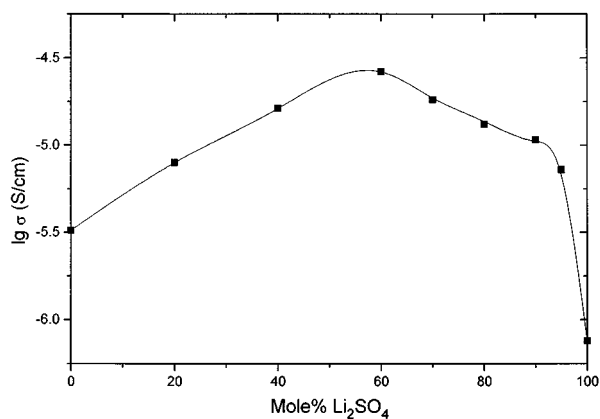


FIG. 3. Experimental data for conductivity vs Li_2SO_4 volume fraction at 350°C for the system $\text{Li}_2\text{SO}_4\text{-Li}_2\text{CO}_3$ (from Dissanayake and Mellander) (Ref. 13).

For example, the knee slightly below the volume fraction 0.7 occurs when the particles touch their nearest neighbors, while the knee slightly above the volume fraction 0.9 occurs when the particles touch their second-nearest neighbors. The model composite with constant radius insulating particles is expected to be closest to the solid salt-alumina mixtures while the model with conducting particles is intended to simulate a system with interface effects between two moderately conducting phases. For this latter model the conductivity is naturally higher than for the other models, but the shape of the curve is very similar to the case of insulating particles. As an example of a system of two moderately conducting phases the conductivity of the $\text{Li}_2\text{SO}_4\text{-Li}_2\text{CO}_3$ system¹³ is shown in Fig. 3. Distinct knees are seen also in this case but it must be kept in mind that this system has a more complicated concentration dependence of the grain size than that used in the models. In this case the grain size has a minimum at the eutectic concentration, 60 mol % Li_2SO_4 , i.e., close to the maximum conductivity.

We note that the assumption of a constant number of particles yields an unphysical asymptotic value for the conductivity as the volume fraction of particles tends to zero. Since the number of particles is kept constant, this limit corresponds to a situation where "spherical particles" of zero radius are surrounded by interface layers of finite size, having higher conductivity than the bulk. The interface layers will thus give an extra contribution to the apparent conductivity.

Figure 4 shows the ionic conductivities for $\text{KNO}_3\text{-Al}_2\text{O}_3$ and $\text{RbNO}_3\text{-Al}_2\text{O}_3$ samples with various compositions. The highest conductivities were obtained at about 58 vol % Al_2O_3 for $\text{KNO}_3\text{-Al}_2\text{O}_3$, and 38 vol % Al_2O_3 for $\text{RbNO}_3\text{-Al}_2\text{O}_3$. It should also be noted that in this figure there is also a minimum value of the conductivity at low alumina concentration. There is no such minimum in Fig. 2. To obtain a minimum and a maximum in the same curve, we accordingly had to assume some other relation between the particle volume fraction and the size of the particles. We found that if we assumed that the particle radius decreases as the volume fraction of particles increases, it is indeed possible to obtain both a minimum and a maximum. For low particle volume fractions, there is not enough interface (or, rather, interphase) to influence the decrease in conductivity

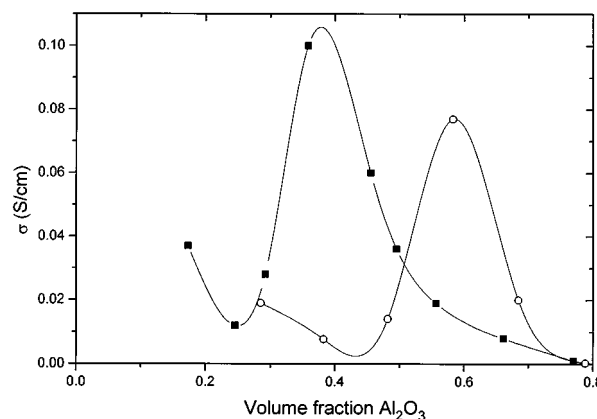


FIG. 4. Experimental data for conductivity vs Al_2O_3 volume fraction at 400°C for the system $\text{RbNO}_3\text{-Al}_2\text{O}_3$ (squares) and $\text{KNO}_3\text{-Al}_2\text{O}_3$ (circles). Note the existence of both a minimum and a maximum at intermediate compositions.

with increasing particle volume fraction in any substantial way, but as the particles become smaller, this tendency is reversed, and a minimum is obtained.

The particle size in these systems actually decreases as the volume fraction of the particle phase increases due to the preparation method used. In such a case the ratio between the thickness of the interface layer and the diameter of the particles increases by a stronger dependence than a proportionality. We thus made a further simulation, assuming that the thickness of the interface layer was proportional to the fifth power of the particle radius (but having the same volume fraction where the particles touch in a bcc lattice as in the previous calculations). We also assumed that the conductivity enhancement in the interphase was lower than in the preceding cases. For comparison, we also performed these calculations for sc and fcc lattices. For those lattices, we have chosen a similar dependence of the ratio between the thickness of the interface layer and the radius of the spheres, with a constant factor yielding the same volumes of interphase at a given volume fraction of particles (for low particle volume fractions).

The results are shown in Fig. 5. We see that the qualita-

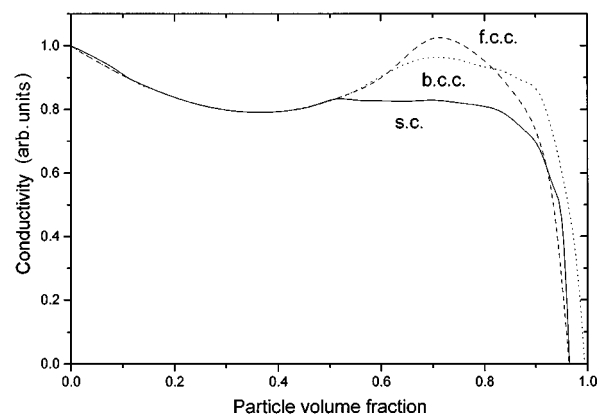


FIG. 5. Results from GCM calculations, assuming that the particles decrease in size with increasing Al_2O_3 volume fraction (as described in the text). We compare results using a sc (solid line), a bcc (dotted line) and a fcc (dashed line) lattice.

tive agreement with experimental results is fairly good. If the spheres do not touch, the exact configuration seems to be of no importance, but as the spheres begin to touch, the type of lattice used has a profound influence on the behavior. For a simple cubic lattice, the peak is situated at a lower concentration of particles (0.52) than for the bcc lattice (0.68), and for a face-centered-cubic lattice, the peak is shifted towards even higher concentrations (0.74). The value of the conductivity maximum also changes; it is higher, the higher the concentration of particles at the maximum. Note also that the finite percolation thresholds are clearly visible.

We can thus assume that the position of the maximum found in experimental data could be used to deduce some information on the structure of the two-phase system. One should note, however, that the shape of the solid particles plays a crucial role, as well as their orientation. For aligned spheroids, or aligned infinite cylinders, the maximum would rather be found at an even higher volume fraction of particles than for an fcc lattice of spheres. For randomly oriented spheroids, one would expect that the position of the maximum is found at an even lower volume fraction than for the sc lattice. This may explain the different positions of the maxima in Fig. 4 and also the difference between the position of the measured and calculated conductivity peak for the solid salt-alumina systems.

It should be stressed that we used a rather crude and *ad hoc* model for the changes in particle size as a function of particle volume fraction (a power law) and it would be interesting to estimate this behavior quantitatively in future work. As the actual dependence is probably different for different systems, it would be interesting to correlate different σ vs insulator volume fraction behaviors to the different particles' size vs insulator volume fraction dependences. It should be noted that the actual form of this dependence can highly influence the maximum value of the conductivity. Of course, the assumed conductivity of the interface layer has an important influence, as well as the assumed stacking of particles.

In addition, we see in Fig. 5 that the minimum in conductivity is shallower than what is obtained experimentally (Fig. 4). Decreasing the conductivity of the interface layer would

make the minimum more accentuated, however, this would also decrease the value of the conductivity maximum. Assuming some distribution of particle sizes would probably have the same effect, as a deviation from monosize distribution would increase the so-called electrical formation factor.³⁶ Having nonspherical particles might also influence the shape of the minimum as it has been shown that deviations from sphericity increase the formation factor.³⁷ The shape of the particles will also influence the position of the maximum.

The peaks also appear rather flattened. This is due to the fact that the grains continue to decrease in size as their volume fraction increases. Using a minimum in grain size may give a better agreement with experiments. Another dependence of the ratio between the thickness of the interface layer and the particle diameter (e.g., having a power higher than five) would alter the shape of the minimum without necessarily decreasing the value in the maximum. Actual measurements on this ratio can give further support for more elaborate assumptions which may yield better agreement with experiments. However, that is beyond the scope of this article.

VI. CONCLUSIONS

The grain consolidation model, in spite of being conceptually simple, provides a good explanation for the conductivity enhancement found in two-phase systems. It also shows some characteristic features in the conductivity versus composition curve, for example the "knees" that are often seen in experimental data. We have also modeled more complicated systems where the grain size is a function of composition and have shown that a conductivity curve with both a minimum and a maximum can be obtained if the size of the grains decreases with increasing volume fraction of grain material.

ACKNOWLEDGMENT

This work has been financially supported by the Swedish Research Council for Engineering Sciences.

¹C. C. Liang, *J. Electrochem. Soc.* **120**, 1289 (1973).

²T. Jow and J. B. Wagner Jr., *J. Electrochem. Soc.* **126**, 1969 (1979).

³P. Hatwig and W. Weppner, *Solid State Ionics* **3/4**, 249 (1982).

⁴K. Shahi and J. B. Goodenough, *J. Solid State Chem.* **42**, 107 (1982).

⁵J. Maier, *J. Phys. Chem. Solids* **46**, 309 (1985).

⁶F. W. Poulsen, in *Transport in Composite Ionic Conductors*, edited by F. W. Poulsen, N. Hessel Andersen, K. Clausen, S. Skaarup, and O. Toft Sørensen (Risø National Laboratory, Roskilde, 1985), p. 67.

⁷A. Bunde, W. Dieterich, and H. E. Roman, *Phys. Rev. Lett.* **55**, 5 (1985).

⁸S. N. Reddy, A. S. Chary, K. Saibabu, and T. Chiranjivi, *Solid State Ionics* **34**, 73 (1989).

⁹L. Q. Chen, in *Materials for Solid State Batteries*, edited by B. V. R. Chowdari and S. Radhakrishna (World Scientific, Singapore, 1986), p. 69.

¹⁰C. W. Nan, *Prog. Mater. Sci.* **37**, 1 (1993).

¹¹S. Jiang and J. B. Wagner Jr., *J. Phys. Chem. Solids* **56**, 1101 (1995); **56**, 1113 (1995).

¹²A. Kumar and K. Shahi, *J. Electrochem. Soc.* **142**, 874 (1995).

¹³M. A. K. L. Dissanayake and B.-E. Mellander, *Solid State Ionics* **21**, 279 (1986).

¹⁴M. H. Waxman and L. J. M. Smits, *Soc. Pet. Eng. J.* **8**, 107 (1968).

¹⁵P.-Z. Wong, J. Koplik, and J. P. Tomanic, *Phys. Rev. B* **30**, 6606 (1984).

¹⁶E. Guyon, L. Oger, and T. J. Plona, *J. Phys. D* **20**, 1637 (1987).

¹⁷P. N. Sen, P. A. Goode, and A. Sibbit, *J. Appl. Phys.* **63**, 4832 (1988).

¹⁸J. Holwech and B. Nøst, *Phys. Rev. B* **39**, 12 845 (1989).

¹⁹Y. Y. Gavronskaya, T. M. Burkat, V. N. Pak, and A. I. Gertsen, *Russ. J. Phys. Chem.* **65**, 1309 (1991).

²⁰D. L. Johnson, J. Koplik, and L. M. Schwartz, *Phys. Rev. Lett.* **57**, 2564 (1986).

- ²¹L. M. Schwartz, E. J. Garboczi, and D. P. Bentz, *J. Appl. Phys.* **78**, 5898 (1995).
- ²²J. N. Roberts and L. M. Schwartz, *Phys. Rev. B* **31**, 5990 (1985).
- ²³L. M. Schwartz and S. Kimminau, *Geophysics* **52**, 1402 (1987).
- ²⁴S. Tyc, L. M. Schwartz, P. N. Sen, and P.-Z. Wong, *J. Appl. Phys.* **64**, 2575 (1988).
- ²⁵B. Nettelblad and G. A. Niklasson, *Solid State Commun.* **90**, 201 (1994).
- ²⁶B. Nettelblad and G. A. Niklasson, in *Proceedings of the DRP '94-Dielectric and Related Phenomena Cracow Institute of Technology, Zakopane, Poland, 1994*, edited by W. Przybylo (Cracow Institute of Technology, Cracow, 1994).
- ²⁷B. Zhu and B.-E. Mellander, *J. Power Sources* **52**, 289 (1994).
- ²⁸B. Zhu and B.-E. Mellander, *Solid State Ionics* **77**, 244 (1995).
- ²⁹S. L. Bryant, D. W. Mellor, and C. A. Cade, *AIChE J.* **39**, 387 (1993).
- ³⁰L. C. Shen, C. Liu, J. Korringa, and K. J. Dunn, *J. Appl. Phys.* **67**, 7071 (1990).
- ³¹C. Liu and L. C. Shen, *J. Appl. Phys.* **73**, 1897 (1993).
- ³²B. Nettelblad and B.-E. Mellander, *IEEE Trans. Dielectrics Electric. Insul.* **3**, 99 (1996).
- ³³B. Sareni, L. Krähenbühl, A. Beroual, and C. Brosseau, *J. Appl. Phys.* **80**, 1688 (1996).
- ³⁴G. K. Batchelor and R. W. O'Brien, *Proc. Roy. Soc. London Ser. A* **355**, 313 (1977).
- ³⁵G. D. Scott and D. M. Kilgour, *J. Phys. D* **2**, 863 (1969).
- ³⁶B. Nettelblad, G. A. Niklasson, B. Åhlén, and R. M. Holt, *J. Phys. D* **28**, 2037 (1995).
- ³⁷P. D. Jackson, D. T. Smith, and P. N. Stanford, *Geophysics* **43**, 1250 (1978).